

# Accepted Manuscript

Structural signatures of igneous sheet intrusion propagation

Craig Magee, James Muirhead, Nick Schofield, Richard J. Walker, Olivier Galland, Simon Holford, Juan Spacapan, Christopher A-L. Jackson, William McCarthy



PII: S0191-8141(18)30382-1

DOI: [10.1016/j.jsg.2018.07.010](https://doi.org/10.1016/j.jsg.2018.07.010)

Reference: SG 3705

To appear in: *Journal of Structural Geology*

Received Date: 21 November 2017

Revised Date: 6 July 2018

Accepted Date: 17 July 2018

Please cite this article as: Magee, C., Muirhead, J., Schofield, N., Walker, R.J., Galland, O., Holford, S., Spacapan, J., Jackson, C.A.-L., McCarthy, W., Structural signatures of igneous sheet intrusion propagation, *Journal of Structural Geology* (2018), doi: 10.1016/j.jsg.2018.07.010.

This is a PDF file of an unedited manuscript that has been accepted for publication. As a service to our customers we are providing this early version of the manuscript. The manuscript will undergo copyediting, typesetting, and review of the resulting proof before it is published in its final form. Please note that during the production process errors may be discovered which could affect the content, and all legal disclaimers that apply to the journal pertain.

# Structural signatures of igneous sheet intrusion propagation

Craig Magee<sup>a\*</sup>, James Muirhead<sup>b</sup>, Nick Schofield<sup>c</sup>, Richard J. Walker<sup>d</sup>, Olivier Galland<sup>e</sup>,  
Simon Holford<sup>f</sup>, Juan Spacapan<sup>g</sup>, Christopher A-L Jackson<sup>a</sup>, William McCarthy<sup>h</sup>

<sup>a</sup>Basins Research Group, Department of Earth Science and Engineering, Imperial College  
London, London, SW7 2BP, UK

<sup>b</sup>Department of Geological Sciences, University of Idaho, Moscow, Idaho, 83844, USA

<sup>c</sup>Geology & Petroleum Geology, School of Geosciences, University of Aberdeen, Aberdeen,  
AB24 3UE, UK

<sup>d</sup>School of Geography, Geology, and the Environment, University of Leicester, Leicester,  
LE1 7RH, UK

<sup>e</sup>Physics of Geological Processes (PGP), The Njord Centre, Department of Geosciences,  
University of Oslo, Blindern, 0316 Oslo, Postbox 1048, Norway

<sup>f</sup>Australian School of Petroleum, University of Adelaide, Adelaide, SA 5005, Australia

<sup>g</sup>Universidad Nacional de La Plata-CONICET-Fundación YPF, 1900 La Plata, Argentina

<sup>h</sup>Department of Earth Sciences, University of St Andrews, St Andrews, KY16 9AL, UK

\*corresponding author: [c.magee@imperial.ac.uk](mailto:c.magee@imperial.ac.uk) (+44 (0)20 7594 6510)

Keywords: Magma; Sheet intrusion; Dyke; Sill; Flow; Structure

## Abstract

The geometry and distribution of planar igneous bodies (i.e. sheet intrusions), such as dykes, sills, and inclined sheets, has long been used to determine emplacement mechanics, define melt source locations, and reconstruct palaeostress conditions to shed light on various

27 tectonic and magmatic processes. Since the 1970's we have recognised that sheet intrusions  
28 do not necessarily display a continuous, planar geometry, but commonly consist of segments.  
29 The morphology of these segments and their connectors is controlled by, and provide insights  
30 into, the behaviour of the host rock during emplacement. For example, tensile brittle  
31 fracturing leads to the formation of intrusive steps or bridge structures between adjacent  
32 segments. In contrast, brittle shear faulting, cataclastic and ductile flow processes, as well as  
33 heat-induced viscous flow or fluidization, promotes magma finger development. Textural  
34 indicators of magma flow (e.g., rock fabrics) reveal that segments are aligned parallel to the  
35 initial sheet propagation direction. Recognising and mapping segment long axes thus allows  
36 melt source location hypotheses, derived from sheet distribution and orientation, to be  
37 robustly tested. Despite the information that can be obtained from these structural signatures  
38 of sheet intrusion propagation, they are largely overlooked by the structural and  
39 volcanological communities. To highlight their utility, we briefly review the formation of  
40 sheet intrusion segments, discuss how they inform interpretations of magma emplacement,  
41 and outline future research directions.

42

### 43 **1. Introduction**

44 Igneous sheet intrusions are broadly planar bodies (e.g., dykes, sills, and inclined sheets) that  
45 facilitate magma flow through Earth's crust. The distribution and geometry of sheet  
46 intrusions is considered to be broadly controlled by the principal stress axes during  
47 emplacement, with intrusion walls typically orienting orthogonal to  $\sigma_3$  within the  $\sigma_1$ - $\sigma_2$  plane,  
48 thus providing a record of syn-emplacement stress conditions (e.g., Anderson, 1936;  
49 Anderson, 1951; Gautneb and Gudmundsson, 1992; Rubin, 1995; Muirhead et al., 2015).  
50 Mapping and analysing the emplacement of igneous sheet swarms therefore allows volcano-  
51 tectonic processes to be unravelled, as well as aiding in identifying magma source locations

52 and palaeogeographic reconstruction (e.g., Anderson, 1936; Walker, 1993; Ernst et al., 1995;  
53 Geshi, 2005). Overall, the link between intrusion geometry and contemporaneous stress field  
54 conditions has underpinned and dominated research and teaching of igneous sheet  
55 emplacement in the fields of structural geology and volcanology.

56 Over the last 50 years, it has been recognised that most igneous sheet intrusions  
57 consist of segments (e.g., Pollard et al., 1975; Delaney and Pollard, 1981; Rickwood, 1990;  
58 Schofield et al., 2012a), similar to structures observed in clastic intrusions (e.g., Vétel and  
59 Cartwright, 2010) and mineralized veins (e.g., Nicholson and Pollard, 1985). Most research  
60 has focused on segmented dykes emplaced via tensile elastic fracturing of the host rock (e.g.,  
61 Delaney and Pollard, 1981; Rickwood, 1990). However, several studies have demonstrated  
62 that mechanisms other than tensile elastic fracturing, such as brittle shear faulting, ductile  
63 flow, and granular flow host rock deformation (e.g., fluidization), can also promote  
64 segmentation of sheet intrusions (e.g., Pollard et al., 1975; Hutton, 2009; Schofield et al.,  
65 2010; Spacapan et al., 2017). Segmentation of igneous sheets is documented over at least five  
66 orders of magnitude in scale, from intrusions that are a few centimetres to hundreds of meters  
67 thick, suggesting that segment formation and linkage are scale independent (Schofield et al.,  
68 2012a). Variable morphologies of segments (e.g., magma fingers; Pollard et al., 1975;  
69 Schofield et al., 2010), as well as those of potential connectors between segments (e.g.,  
70 intrusive steps, broken bridges; Rickwood, 1990), characterise the broader sheet geometry  
71 and reflect the mechanical processes that facilitate emplacement (Schofield et al., 2012a).  
72 Rock fabric analyses of primary magma flow structures (e.g., chilled margin magnetic  
73 fabrics) have shown that the long axes of segments and their connectors are typically parallel  
74 to the direction of initial sheet propagation (e.g., Baer and Reches, 1987; Rickwood, 1990;  
75 Baer, 1995; Liss et al., 2002; Magee et al., 2012; Hoyer and Watkeys, 2017). Identification  
76 and analysis of segments and connectors in the field and in seismic reflection data thus

77 provides a simple way to map primary magma propagation patterns and determine syn-  
78 emplacement host rock behaviour (e.g., Rickwood, 1990; Hansen et al., 2004; Thomson and  
79 Hutton, 2004; Trude et al., 2004; Schofield et al., 2012a; Schofield et al., 2012b). Here, our  
80 aim is to: (i) summarise our current understanding of magma segment formation and sheet  
81 intrusion; (ii) highlight how these structures can be used to unravel controls on magma flow  
82 through sheet intrusions in Earth's crust; and (iii) outline future research directions and  
83 implications for the study of sheet intrusion emplacement.

84

## 85 **2. Primary magma flow indicators**

86

### 87 *2.1. Intrusive steps and bridge structures formed by tensile brittle fracturing*

88 Regardless of their orientation or propagation direction, many sheet intrusions exhibit a  
89 stepped geometry consisting of sub-parallel segments that are slightly offset from one another  
90 and may overlap (Figs 1-3) (e.g., Delaney and Pollard, 1981; Rickwood, 1990; Schofield et  
91 al., 2012a). It is broadly accepted that stepped intrusion geometries result from segmentation  
92 of a propagating tensile elastic fracture, i.e. oriented orthogonal to  $\sigma_3$ , immediately ahead of  
93 an advancing sheet intrusion (e.g., Delaney and Pollard, 1981; Baer, 1995). As magma fills  
94 the fracture, segments begin to inflate and widen through lateral tip propagation, promoting  
95 tensile fracture of the intervening host rock and eventual segment coalescence (Fig. 1A) (e.g.,  
96 Rickwood, 1990; Hutton, 2009; Schofield et al., 2012a). Structural signatures of this  
97 segmentation are controlled by segment offset, which describes the strike-perpendicular  
98 distance between the planes of two segments, and overlap, which can be negative (i.e.  
99 underlap) and describes the strike-parallel distance between segment tips (Fig. 1A) (cf.  
100 Delaney and Pollard, 1981; Rickwood, 1990). We also introduce 'stepping direction', which

101 can either be consistent or inconsistent, to define the relative offset direction of adjacent  
102 segments (Fig. 1B).

103

104 Insert Figure 1

105

106 When viewed in a 2D cross-section (e.g., an outcrop), segments typically appear  
107 unconnected at their distal end, away from the magma source, whereas increased magma  
108 supply in proximal locations promotes their inflation and coalescence to form a continuous  
109 sheet intrusion (Fig. 1A) (Rickwood, 1990; Schofield et al., 2012a; Schofield et al., 2012b).  
110 Connectors between segments are classified as intrusive steps, if the segment overlap is  
111 neutral or negative, or bridge structures when segments overlap (Figs 1-3). Changes in  
112 overlap along segment long axes may mean steps transition into bridge structures and vice  
113 versa (Schofield et al., 2012a; Schofield et al., 2012b). Variations in the degree and style of  
114 segment connectivity with distance from the magma source imply that the segmentation  
115 process results from initial sheet propagation dynamics (Schofield et al., 2012a).

116

117 Insert Figures 2 and 3

118

### 119 *2.1.1. Fracture segmentation*

120 Two processes are commonly invoked to explain the development of initially unconnected  
121 fracture segments: (i) syn-emplacement rotation of the principal stress axes orientations (e.g.,  
122 Pollard et al., 1982; Nicholson and Pollard, 1985; Takada, 1990); and (ii) exploitation of  
123 preferentially oriented, pre-existing structures (e.g., Hutton, 2009; Schofield et al., 2012a;  
124 Stephens et al., 2017). Geological systems likely display a combination of these segmentation

125 mechanisms, and potentially others, so it is therefore important to understand the  
126 characteristics of each process to decipher their relative contributions.

127         In the first scenario, a change in the principal stress axes orientation ahead of a  
128 propagating fracture, likely due to the onset of mixed mode loading (mode I+II or mode  
129 I+III), causes it to twist and split into en-echelon segments that strike orthogonal to the  
130 locally reoriented  $\sigma_3$  axis (Fig. 4A) (Pollard et al., 1982; Nicholson and Pollard, 1985; Cooke  
131 et al., 1999). This segmentation of mixed mode fractures is dictated by the maximum  
132 circumferential stress direction, direction of maximum energy release, maximum principal  
133 stress, direction of strain energy minimum, and the symmetry criterion (Cooke et al., 1999).  
134 The plane broadly defined by the overall geometry of the en-echelon segments remains  
135 parallel to the orientation of the original fracture (Fig 4A) (Rickwood, 1990). Steps and  
136 bridge structures generated due to this style of segmentation have a consistent stepping  
137 direction (e.g., Fig. 1B).

138

139 Insert Figure 4

140

141         The second mechanism for step and bridge formation involves exploitation of  
142 preferentially oriented (i.e. with respect to the contemporaneous principal stress axes), pre-  
143 existing structures by propagating fractures/intrusions (e.g., Hutton, 2009; Schofield et al.,  
144 2012a; Stephens et al., 2017). For example, many sills emplaced into sedimentary strata can  
145 be divided into segments that exploited different bedding planes in an attempt to find the least  
146 resistant pathway (e.g., Figs 2D and 3A) (Hutton, 2009). Bedding planes are particularly  
147 exploited because they: (i) exhibit relatively lower tensile strength and fracture toughness  
148 compared to intact rock (e.g., Schofield et al., 2012a; Kavanagh and Pavier, 2014; Kavanagh  
149 et al., 2017); and/or (ii) mark a significant mechanical contrast in intact rock properties (e.g.,

150 Poisson's ratio, Young's modulus) that localises strain (e.g., Kavanagh et al., 2006;  
151 Gudmundsson, 2011). In contrast to en-echelon segments, the stepping direction of intrusions  
152 exploiting different pre-existing weaknesses may be inconsistent (Figs 1B and 3E) (Schofield  
153 et al., 2012a).

154         Alternative mechanisms that may account for segmentation and step formation  
155 involve: (i) development of high stress intensities at the leading edge of an intruding sheet,  
156 promoting rapid crack propagation and formation of a fracture morphology, with a consistent  
157 stepping direction, akin to hackle marks (Fig. 4B) (Schofield et al., 2012a); or (ii) the  
158 occurrence of low or zero fracture toughness, pre-existing structures (e.g., faults), striking  
159 orthogonal to the sheet propagation direction, which can promote segmentation and provide a  
160 pathway for magma to form a fault-parallel step (Magee et al., 2013; Stephens et al., 2017).  
161 The stepping direction of sills influenced by pre-existing faults is controlled by the fault dip  
162 direction relative to the sheet propagation direction (Magee et al., 2013). In these scenarios,  
163 the stepped fracture plane is continuous and thus allows the magma to propagate as a single  
164 sheet; bridge structures cannot form via these processes because segments do not overlap  
165 (e.g., Fig. 1B).

166

#### 167 *2.1.2. Host rock deformation and bridge development*

168 When segments overlap, their inflation may be accommodated by bending of the intervening  
169 host rock bridge (Figs 1A, 3A, and B) (Farmin, 1941; Nicholson and Pollard, 1985;  
170 Rickwood, 1990; Hutton, 2009). The monoformal folding of the host rock bridge records a  
171 tangential longitudinal strain relative to the orientation of the folded layers and induces outer-  
172 arc extension and inner-arc compression along the fold convex and concave surfaces,  
173 respectively (Hutton, 2009; Schofield et al., 2012a). As magma inflation continues, outer-arc  
174 extension increases and may exceed the tensile strength of the intact host rock, promoting



175 development of extension fractures across the bridge (Figs 3B and C) (e.g., Hutton, 2009;  
176 Schofield et al., 2012b). Fractures cross-cutting unfolded bridge structures may also form if  
177 local crack-inducing stresses at segment tips are sufficiently high to promote fracture rotation  
178 and propagation towards each other (e.g., Fig. 3D) (e.g., Olson and Pollard, 1989). Continued  
179 fracture growth and infilling by magma can separate the bridge from one or both sides to  
180 form a broken bridge (Fig. 3B) or a bridge xenolith (Fig. 3D), respectively (Hutton, 2009).

181

## 182 *2.2. Magma finger formation through brittle and/or non-brittle processes*

183 In contrast to established tensile brittle fracturing models, several studies have demonstrated  
184 that magma may intrude via brittle faulting, cataclastic flow, or non-brittle processes (e.g.,  
185 Pollard et al., 1975; Duffield et al., 1986; Schofield et al., 2010; Schofield et al., 2012a;  
186 Wilson et al., 2016). Such host rock deformation modes lead to the emplacement of magma  
187 fingers; i.e. long, linear or sinuous, narrow segments that have blunt and/or bulbous  
188 terminations (e.g., Pollard et al., 1975; Schofield et al., 2010; Schofield et al., 2012a;  
189 Spacapan et al., 2017).

190 Sheet intrusion into unconsolidated or highly incompetent host rocks, where little  
191 cohesion between grains and/or low shear moduli inhibits tensile brittle failure, can instigate  
192 magma finger formation (e.g., Pollard et al., 1975; Schofield et al. 2012a). For example,  
193 accommodation of magma by pore collapse and cataclastic flow can affect sheet intrusions  
194 emplaced: (i) at shallow-levels in sedimentary basins where host rock sequences have  
195 undergone little burial and/or diagenesis (e.g., Einsele et al., 1980; Morgan et al., 2008;  
196 Schofield et al., 2012a); or (ii) in strata that have been prevented from undergoing normal  
197 compaction with burial (Eide et al., 2017). Observed pegmatite bead-strings, which appear  
198 similar to magma fingers, formed during syn- or post-metamorphism and emplaced into hot,

199 incompetent rocks suggests high ambient host rock temperatures can promote ductile host  
200 rock deformation and magma finger formation (cf. Bons et al., 2004).

201 Shear failure of unconsolidated and relatively soft (e.g., shale) host rock by brittle  
202 faulting and/or ductile deformation can also form and accommodate magma fingers (Fig. 5)  
203 (e.g., Pollard, 1973; Duffield et al., 1986; Rubin, 1993; Spacapan et al., 2017). For example,  
204 kinematic indicators of such compressional shear structures adjacent to magma fingers in the  
205 Neuquen Basin, Argentina, indicate that the intrusion ‘pushed’ into the host rock, leading to  
206 confined rock wedging (Fig. 5) (Pollard, 1973; Rubin, 1993; Spacapan et al., 2017). This  
207 hybrid propagation mechanism, called viscous indentation, is assumed to occur when the  
208 viscous shear stresses within a flowing magma, near its intrusion tip, are transferred to and  
209 promote shear failure of the host rock (Galland et al., 2014). Viscous indentation is therefore  
210 expected to primarily accommodate emplacement of viscous magma (Donnadiou and Merle,  
211 1998; Merle and Donnadiou, 2000).

212

213 Insert Figure 5

214

215 Intrusion-induced heating (i.e. primary non-brittle emplacement) can cause some host  
216 rocks, particularly evaporites and bituminous coals, to behave as high viscosity fluids (i.e.  
217 fluidisation), the viscous deformation of which allows low viscosity melt injections to form  
218 magma fingers (e.g., Fig. 6) (Schofield et al., 2010; Schofield et al., 2012a; Schofield et al.,  
219 2014). Magma fingers can also form by fluidization (i.e. granular flow) of coherent,  
220 mechanically competent host rock (e.g., Pollard et al., 1975; Schofield et al. 2012a); i.e.  
221 secondary induced non-brittle magma emplacement (Schofield et al., 2012a). Two secondary  
222 induced non-brittle emplacement scenarios may be considered whereby magma intrusion can:  
223 (i) promote *in situ* boiling and volatisation of pore-fluids via heating (i.e. thermal

224 fluidization); or (ii) open fractures that rapidly depressurize pore-fluids, which expand and  
225 catastrophically disaggregate the host rock (Schofield et al., 2010; Schofield et al., 2012a).

226

227 Insert Figure 6

228

### 229 **3. Discussion**

230 Having described how segmentation occurs and is structurally accommodated, here we  
231 discuss selected examples of how this knowledge has been applied and highlight possible  
232 future directions.

233

#### 234 *3.1. Lateral magma flow in mafic sill-complexes*

235 The current paradigm describing crustal magma transport broadly involves the vertical ascent  
236 and/or lateral intrusion of dykes (e.g., Gudmundsson, 2006; Cashman and Sparks, 2013).

237 However, recent field- and seismic-based studies that infer magma flow patterns from  
238 segment long axes and/or rock fabric analyses within interconnected networks of mafic sills  
239 and inclined sheets (i.e. sill-complexes), demonstrate that these systems can facilitate  
240 significant vertical (up to 12 km) and lateral (up to 4000 km) magma transport (e.g.,  
241 Cartwright and Hansen, 2006; Leat, 2008; Muirhead et al., 2014; Magee et al., 2016). The  
242 lateral growth of such sill-complexes has been shown to control vent migrations and,  
243 potentially, transitions from effusive to explosive volcanism in active and extinct mafic  
244 monogenetic volcanic fields (e.g., Kavanagh et al., 2015; Muirhead et al., 2016). Mapping  
245 segment long axes suggests that sill-complexes may be as important as dykes in various  
246 tectonic, magmatic, and volcanic processes (Magee et al., 2016).

247

#### 248 *3.2. Intrusion opening vectors*

249 Over a century of research has led to the prescribed dogma that sheet opening exclusively  
250 involves tensile dilation of Mode I fractures (e.g., Anderson, 1936). Intrusion planes are  
251 therefore expected to orient orthogonal to  $\sigma_3$ , which is a function of the interplay between far-  
252 field and local stress fields (e.g., Anderson, 1936; Anderson, 1951; Odé, 1957; Gautneb and  
253 Gudmundsson, 1992; Geshi, 2005). However, from analysing sheet segmentation processes,  
254 it is clear that several brittle and non-brittle processes can accommodate the emplacement of  
255 sheet intrusions that may not orient orthogonal to  $\sigma_3$  (e.g., Schofield et al., 2012a; Schofield  
256 et al., 2014). Although often overlooked, it is therefore important to test the validity of the  
257 assumed relationship between the orientation of intrusive sheets and  $\sigma_3$ , through analysis of  
258 intrusion opening vectors (e.g., Walker, 1993; Jolly and Sanderson, 1997; Walker, 2016;  
259 Walker et al., 2017). Importantly, the geometry of segment connectors provides a record of  
260 local intrusion opening vectors (e.g., Olson and Pollard, 1989; Walker, 1993; Jolly and  
261 Sanderson, 1995; Cooke and Pollard, 1996; Stephens et al., 2017; Stephens et al., 2018).  
262 Steps formed during pure tensile opening of parallel magma segments should have virtually  
263 zero thickness and simply accommodate shear displacement on a plane orthogonal to the  
264 sheet intrusion plane (e.g., Figs 2A and C) (e.g., Stephens et al., 2017). Conversely, thick  
265 steps require an opening vector that was *not* orthogonal to the intrusion plane (e.g., Fig. 2D)  
266 (Walker et al., 2017). Whilst opening vectors of individual connectors may largely reflect  
267 local stress fields related to crack-tip processes (e.g., Olson and Pollard, 1989), identifying  
268 and collating such opening vector measurements across a sheet intrusion swarm can provide a  
269 more robust test of the syn-emplacement stress conditions than analyses of sheet orientation  
270 alone (Jolly and Sanderson, 1997; Walker et al., 2017). In particular, cataloguing opening  
271 vectors of segments within a sheet intrusion complex may help determine whether variably-  
272 oriented intrusions can be prescribed to single or multiple stress states. For example, although  
273 sill segments within the San Rafael Sub-Volcanic Field, USA range in dip from  $\sim 50^\circ$  SE to

274 ~40° NW, all record vertical opening vectors that indicate emplacement of the entire complex  
275 occurred within a single stress state (Stephens et al., 2018).

276

### 277 *3.3. Bridge structures and relay zones*

278 As with intrusions, faults and fractures grow through stages of nucleation and linkage of  
279 multiple discontinuous segments (e.g., Cartwright et al., 1996; Walsh et al., 2003). The  
280 amount of overlap and offset of fault or fracture segments, and the existence of pre-existing  
281 structure, leads to different styles of deformation in the intervening *relay zone* that  
282 accommodates displacement gradients between fault segments (e.g., Tentler and Acocella,  
283 2010). Despite the apparent similarity of relay zones and bridge structures (Schofield et al.,  
284 2012b), few comparisons exist between the resulting ancillary structures associated with  
285 segmented faults and segmented intrusions. Whilst relay zones have received considerable  
286 attention in the literature (e.g., Peacock and Sanderson, 1991; Long and Imber, 2011), to our  
287 knowledge there is no catalogue of overlap, offset, and strain parameters for bridge  
288 structures. We suggest that systematic study of bridge structures, and comparison to relay  
289 zones, could yield important constraints on shared processes.

290

## 291 **4. Conclusion**

292 Igneous sheet intrusions are not necessarily emplaced as continuous, planar bodies but  
293 commonly develop through the coalescence of discrete magma segments. Segmentation can  
294 be primarily attributed to either: (i) splitting of a tensile brittle fracture propagating ahead of a  
295 sheet intrusion due to stress field rotations or exploitation of pre-existing weaknesses; (ii)  
296 brittle shear and flow (i.e. pore collapse) deformation of poorly consolidated host rocks;  
297 and/or (iii) non-brittle host rock fluidization. By briefly reviewing advances in our  
298 understanding of sheet intrusion growth, we demonstrate how different emplacement

299 processes produce a variety of segment morphologies (e.g., magma fingers) and connecting  
300 structures (e.g., steps and bridge structures), the long axes of which record the initial  
301 fracture/magma propagation dynamics. We highlight how mapping of sheet segments and  
302 analysing their formation can provide important clues regarding the distribution of melt  
303 sources, how magma transits Earth's crust, mechanics of intrusion-induced host rock  
304 deformations, and palaeostress states in various volcanic-tectonic environments.

305

## 306 **5. Acknowledgments**

307 CM acknowledges a Junior Research Fellowship funded by Imperial College London. JDM  
308 acknowledges National Science Foundation grant EAR-1654518. Ken McCaffrey, Paul Bons,  
309 and Sandy Cruden are thanked for their constructive reviews.

310

## 311 **6. Figure Captions**

312 Figure 1: (A) Schematic diagram documenting the description and development of segments  
313 connected by steps and bridge structures (modified from Magee et al., 2016). Note the  
314 monoformal folding of bridge structures. (B) Schematic diagram defining consistent and  
315 inconsistent stepping directions.

316

317 Figure 2: Steps developed in mafic sheets intruding: (A and B) Mesozoic limestone and shale  
318 metasedimentary rocks on Ardnamurchan, NW Scotland; (C) Neoproterozoic schists at  
319 Mallaig, NW Scotland; and (D) a sedimentary succession on Axel Heiburg island, Canada  
320 (photo courtesy of Martin Jackson).

321

322 Figure 3: Different bridge structures recorded in mafic intrusions into: (A) Beacon  
323 Supergroup sedimentary strata along the Theron Mountains, Antarctica (modified from

324 Hutton, 2009); (B) Beacon Supergroup sedimentary strata along the Allan Hills, Antarctica;  
325 (C) a massive dolerite intrusion on Ardnamurchan, NW Scotland; and (D) Mesozoic  
326 limestone and shale metasedimentary rocks on Ardnamurchan, NW Scotland. (E) Opacity  
327 render of a sill in the Flett Basin, NE Atlantic and corresponding seismic sections detailing  
328 intrusive step and bridge growth along i-iv segment boundaries (modified from Schofield et  
329 al., 2012b); note that it can be difficult to determine where segments are bounded by steps or  
330 bridge structures in seismic reflection data.

331

332 Figure 4: (A) Schematic showing how a change in the principal stress axes can segment a  
333 propagating sheet (after Hutton, 2009). (B) Hackle marks developed on a joint plane  
334 (redrawn from Kulander et al., 1979).

335

336 Figure 5: Small-scale imbricate fold and thrust duplex developed due to viscous indentation  
337 of finger-like sill intrusions in the Neuquén Basin, Argentina (modified from Spacapan et al.,  
338 2017).

339

340 Figure 6: (A and B) Magma fingers developed in response to intrusion-induced heating and  
341 plastic deformation of the host rock coals in the Raton Basin, Colorado (modified from  
342 Schofield et al., 2012a). (C) Schematic diagrams showing the simplified 3D morphology of  
343 the magma fingers in (A and B) (Schofield, 2009).

344

## 345 **7. References**

346 Anderson, E.M., 1936. Dynamics of formation of cone-sheets, ring-dykes, and cauldron  
347 subsidence. *Proceedings of the Royal Society of Edinburgh* 56, 128-157.

- 348 Anderson, E.M., 1951. The dynamics of faulting and dyke formation with applications to  
349 Britain. Oliver and Boyd, Edinburgh, 206 pp.
- 350 Baer, G., 1995. Fracture propagation and magma flow in segmented dykes: field evidence  
351 and fabric analyses, Makhtesh Ramon, Israel. Physics and chemistry of dykes. Balkema,  
352 Rotterdam, 125-140.
- 353 Baer, G., Reches, Z.E., 1987. Flow patterns of magma in dikes, Makhtesh Ramon, Israel.  
354 Geology 15, 569-572.
- 355 Cartwright, J.A., Hansen, D.M., 2006. Magma transport through the crust via interconnected  
356 sill complexes. Geology 34, 929-932.
- 357 Cartwright, J.A., Mansfield, C., Trudgill, B., 1996. The growth of normal faults by segment  
358 linkage. In: Buchanan, P.G., Nieuwland, D.A., (eds), Modern Developments in Structural  
359 Interpretation, Validation and Modelling. Geological Society, London, Special Publications  
360 99, 163-177.
- 361 Cashman, K.V., Sparks, R.S.J., 2013. How volcanoes work: A 25 year perspective.  
362 Geological Society of America Bulletin 125, 664-690.
- 363 Cooke, M.L., Mollema, P.N., Pollard, D.D., Aydin, A., 1999. Interlayer slip and joint  
364 localization in the East Kaibab Monocline, Utah: field evidence and results from numerical  
365 modelling. Geological Society, London, Special Publications 169, 23-49.
- 366 Cooke, M.L., Pollard, D.D., 1996. Fracture propagation paths under mixed mode loading  
367 within rectangular blocks of polymethyl methacrylate. Journal of Geophysical Research:  
368 Solid Earth 101, 3387-3400.
- 369 Delaney, P.T., Pollard, D.D., 1981. Deformation of host rocks and flow of magma during  
370 growth of minette dikes and breccia-bearing intrusions near Ship Rock, New Mexico. US  
371 Geological Survey Professional Paper 1202, 61 pp.



- 372 Donnadieu, F., Merle, O., 1998. Experiments on the indentation process during cryptodome  
373 intrusions: new insights into Mount St. Helens deformation. *Geology* 26, 79-82.
- 374 Duffield, W.A., Bacon, C.R., Delaney, P.T., 1986. Deformation of poorly consolidated  
375 sediment during shallow emplacement of a basalt sill, Coso Range, California. *Bull Volcanol*  
376 48, 97-107.
- 377 Eide, C.H., Schofield, N., Jerram, D.A., Howell, J.A., 2017. Basin-scale architecture of  
378 deeply emplaced sill complexes: Jameson Land, East Greenland. *Journal of the Geological*  
379 *Society* 174, 23-40.
- 380 Einsele, G., Gieskes, J.M., Curray, J., Moore, D.M., Aguayo, E., Aubry, M.-P., Fornari, D.,  
381 Guerrero, J., Kastner, M., Kelts, K., 1980. Intrusion of basaltic sills into highly porous  
382 sediments, and resulting hydrothermal activity. *Nature* 283, 441-445.
- 383 Ernst, R., Head, J., Parfitt, E., Grosfils, E., Wilson, L., 1995. Giant radiating dyke swarms on  
384 Earth and Venus. *Earth-Science Reviews* 39, 1-58.
- 385 Farmin, R., 1941. Host-rock inflation by veins and dikes at Grass Valley, California.  
386 *Economic Geology* 36, 143-174.
- 387 Galland, O., Burchardt, S., Hallot, E., Mourgues, R., Bulois, C., 2014. Dynamics of dikes  
388 versus cone sheets in volcanic systems. *Journal of Geophysical Research: Solid Earth* 119,  
389 6178-6192.
- 390 Gautneb, H., Gudmundsson, A., 1992. Effect of local and regional stress fields on sheet  
391 emplacement in West Iceland. *Journal of Volcanology and Geothermal Research* 51, 339-  
392 356.
- 393 Geshi, N., 2005. Structural development of dike swarms controlled by the change of magma  
394 supply rate: the cone sheets and parallel dike swarms of the Miocene Otoge igneous complex,  
395 Central Japan. *Journal of Volcanology and Geothermal Research* 141, 267-281.

- 396 Gudmundsson, A., 2006. How local stresses control magma-chamber ruptures, dyke  
397 injections, and eruptions in composite volcanoes. *Earth-Science Reviews* 79, 1-31.
- 398 Gudmundsson, A., 2011. Deflection of dykes into sills at discontinuities and magma-chamber  
399 formation. *Tectonophysics* 500, 50-64.
- 400 Hansen, D.M., Cartwright, J.A., Thomas, D., 2004. 3D seismic analysis of the geometry of  
401 igneous sills and sill junction relationships. In: Davies, R.J., Cartwright, J.A., Stewart, S.A.,  
402 Lappin, M., Underhill, J.R., (eds), *3D seismic technology: Application to the exploration of*  
403 *sedimentary basins*, Geological Society, London, *Memoirs* 29, 199-208.
- 404 Hoyer, L., Watkeys, M.K., 2017. Using magma flow indicators to infer flow dynamics in  
405 sills. *Journal of Structural Geology* 96, 161-175.
- 406 Hutton, D.H.W., 2009. Insights into magmatism in volcanic margins: bridge structures and a  
407 new mechanism of basic sill emplacement - Theron Mountains, Antarctica. *Petroleum*  
408 *Geoscience* 15, 269-278.
- 409 Jolly, R., Sanderson, D., 1997. A Mohr circle construction for the opening of a pre-existing  
410 fracture. *Journal of Structural Geology* 19, 887-892.
- 411 Jolly, R., Sanderson, D.J., 1995. Variation in the form and distribution of dykes in the Mull  
412 swarm, Scotland. *Journal of Structural Geology* 17, 1543-1557.
- 413 Kavanagh, J.L., Boutelier, D., Cruden, A., 2015. The mechanics of sill inception, propagation  
414 and growth: Experimental evidence for rapid reduction in magmatic overpressure. *Earth and*  
415 *Planetary Science Letters* 421, 117-128.
- 416 Kavanagh, J.L., Menand, T., Sparks, R.S.J., 2006. An experimental investigation of sill  
417 formation and propagation in layered elastic media. *Earth and Planetary Science Letters* 245,  
418 799-813.
- 419 Kavanagh, J.L., Pavier, M.J., 2014. Rock interface strength influences fluid-filled fracture  
420 propagation pathways in the crust. *Journal of Structural Geology* 63, 68-75.

- 421 Kavanagh, J.L., Rogers, B.D., Boutelier, D., Cruden, A.R., 2017. Controls on sill and dyke-  
422 sill hybrid geometry and propagation in the crust: The role of fracture toughness.  
423 *Tectonophysics* 698, 109-120.
- 424 Kulander, B.R., Barton, C.C., Dean, S.L., 1979. Application of fractography to core and  
425 outcrop fracture investigations. Department of Energy, Morgantown, WV (USA).  
426 Morgantown Energy Research Center.
- 427 Leat, P.T., 2008. On the long-distance transport of Ferrar magmas. Geological Society,  
428 London, Special Publications 302, 45-61.
- 429 Liss, D., Hutton, D.H., Owens, W.H., 2002. Ropy flow structures: A neglected indicator of  
430 magma-flow direction in sills and dikes. *Geology* 30, 715-718.
- 431 Long, J.J., Imber, J., 2011. Geological controls on fault relay zone scaling. *Journal of*  
432 *Structural Geology* 33, 1790-1800.
- 433 Magee, C., Jackson, C.A.-L., Schofield, N., 2013. The influence of normal fault geometry on  
434 igneous sill emplacement and morphology. *Geology* 41, 407-410.
- 435 Magee, C., Muirhead, J.D., Karvelas, A., Holford, S.P., Jackson, C.A., Bastow, I.D.,  
436 Schofield, N., Stevenson, C.T., McLean, C., McCarthy, W., 2016. Lateral magma flow in  
437 mafic sill complexes. *Geosphere* 12, 809-841.
- 438 Magee, C., Stevenson, C., O'Driscoll, B., Schofield, N., McDermott, K., 2012. An alternative  
439 emplacement model for the classic Ardnamurchan cone sheet swarm, NW Scotland,  
440 involving lateral magma supply via regional dykes. *Journal of Structural Geology* 43, 73-91.
- 441 Merle, O., Donnadiou, F., 2000. Indentation of volcanic edifices by the ascending magma. In:  
442 Vendeville, B., Mart, Y., Vigneresse, J.-L., (eds), *Salt, Shale and Igneous Diapirs in and*  
443 *around Europe*. Geological Society, London, Special Publications 174, 43-53.

- 444 Morgan, S., Stanik, A., Horsman, E., Tikoff, B., de Saint Blanquat, M., Habert, G., 2008.  
445 Emplacement of multiple magma sheets and wall rock deformation: Trachyte Mesa intrusion,  
446 Henry Mountains, Utah. *Journal of Structural Geology* 30, 491-512.
- 447 Muirhead, J.D., Airoidi, G., White, J.D., Rowland, J.V., 2014. Cracking the lid: Sill-fed dikes  
448 are the likely feeders of flood basalt eruptions. *Earth and Planetary Science Letters* 406, 187-  
449 197.
- 450 Muirhead, J.D., Kattenhorn, S.A., Le Corvec, N., 2015. Varying styles of magmatic strain  
451 accommodation across the East African Rift. *Geochemistry, Geophysics, Geosystems* 16,  
452 2775-2795.
- 453 Muirhead, J.D., Van Eaton, A.R., Re, G., White, J.D., Ort, M.H., 2016. Monogenetic  
454 volcanoes fed by interconnected dikes and sills in the Hopi Buttes volcanic field, Navajo  
455 Nation, USA. *Bulletin of Volcanology* 78, 11.
- 456 Nicholson, R., Pollard, D., 1985. Dilation and linkage of echelon cracks. *Journal of Structural*  
457 *Geology* 7, 583-590.
- 458 Odé, H., 1957. Mechanical Analysis of the Dike Pattern of the Spanish Peaks Area, Colorado.  
459 *Geological Society of America Bulletin* 68, 567.
- 460 Olson, J., Pollard, D.D., 1989. Inferring paleostresses from natural fracture patterns: A new  
461 method. *Geology* 17, 345-348.
- 462 Peacock, D., Sanderson, D., 1991. Displacements, segment linkage and relay ramps in normal  
463 fault zones. *Journal of Structural Geology* 13, 721-733.
- 464 Pollard, D.D., 1973. Derivation and evaluation of a mechanical model for sheet intrusions.  
465 *Tectonophysics* 19, 233-269.
- 466 Pollard, D.D., Muller, O.H., Dockstader, D.R., 1975. The form and growth of fingered sheet  
467 intrusions. *Geological Society of America Bulletin* 86, 351-363.

- 468 Pollard, D.D., Segall, P., Delaney, P.T., 1982. Formation and interpretation of dilatant  
469 echelon cracks. *Geological Society of America Bulletin* 93, 1291-1303.
- 470 Rickwood, P., 1990. The anatomy of a dyke and the determination of propagation and magma  
471 flow directions. In: Parker, A.J., Rickwood, P.C., Tucker, D.H., (eds), *Mafic dykes and*  
472 *emplacement mechanisms*, Balkema, Rotterdam, 81-100.
- 473 Rubin, A.M., 1993. Tensile fracture of rock at high confining pressure: implications for dike  
474 propagation. *Journal of Geophysical Research: Solid Earth* 98, 15919-15935.
- 475 Rubin, A.M., 1995. Propagation of magma-filled cracks. *Annual Review of Earth and*  
476 *Planetary Sciences* 23, 287-336.
- 477 Schofield, N., 2009. Linking sill morphology to emplacement mechanisms. PhD thesis.  
478 University of Birmingham.
- 479 Schofield, N., Alsop, I., Warren, J., Underhill, J.R., Lehné, R., Beer, W., Lukas, V., 2014.  
480 Mobilizing salt: Magma-salt interactions. *Geology* 42, 599-602.
- 481 Schofield, N., Heaton, L., Holford, S.P., Archer, S.G., Jackson, C.A.-L., Jolley, D.W., 2012b.  
482 Seismic imaging of 'broken bridges': linking seismic to outcrop-scale investigations of  
483 intrusive magma lobes. *Journal of the Geological Society* 169, 421-426.
- 484 Schofield, N., Stevenson, C., Reston, T., 2010. Magma fingers and host rock fluidization in  
485 the emplacement of sills. *Geology* 38, 63-66.
- 486 Schofield, N.J., Brown, D.J., Magee, C., Stevenson, C.T., 2012a. Sill morphology and  
487 comparison of brittle and non-brittle emplacement mechanisms. *Journal of the Geological*  
488 *Society* 169, 127-141.
- 489 Spacapan, J.B., Galland, O., Leanza, H.A., Planke, S., 2017. Igneous sill and finger  
490 emplacement mechanism in shale-dominated formations: a field study at Cuesta del  
491 Chihuido, Neuquén Basin, Argentina. *Journal of the Geological Society* 174, 422-433.

- 492 Stephens, T.L., Walker, R.J., Healy, D., Bubeck, A., England, R., McCaffrey, K., 2017.  
493 Igneous sills record far-field and near-field stress interactions during volcano construction:  
494 Isle of Mull, Scotland. *Earth and Planetary Science Letters* 478, 159-174.
- 495 Stephens, T.L., Walker, R.J., Healy, D., Bubeck, A., England, R.W., 2018. Mechanical  
496 models to estimate the paleostress state from igneous intrusions. *Solid Earth* (in press).
- 497 Takada, A., 1990. Experimental study on propagation of liquid-filled crack in gelatin: Shape  
498 and velocity in hydrostatic stress condition. *Journal of Geophysical Research: Solid Earth* 95,  
499 8471-8481.
- 500 Tentler, T., Acocella, V., 2010. How does the initial configuration of oceanic ridge segments  
501 affect their interaction? Insights from analogue models. *Journal of Geophysical Research:*  
502 *Solid Earth* 115, B01401.
- 503 Thomson, K., Hutton, D., 2004. Geometry and growth of sill complexes: insights using 3D  
504 seismic from the North Rockall Trough. *Bulletin of Volcanology* 66, 364-375.
- 505 Trude, K.J., 2004. Kinematic Indicators for Shallow Level Igneous Intrusions from 3D  
506 Seismic Data: Evidence of Flow Direction and Feeder Location. In: Davies, R.J., Cartwright,  
507 J.A., Stewart, S.A., Lappin, M., Underhill, J.R., (eds), *3D seismic technology: Application to*  
508 *the exploration of sedimentary basins*, Geological Society, London, *Memoirs* 29, 209-218.
- 509 Vétel, W., Cartwright, J., 2010. Emplacement mechanics of sandstone intrusions: insights  
510 from the Panoche Giant Injection Complex, California. *Basin Research* 22, 783-807.
- 511 Walker, G.P.L., 1993. Re-evaluation of inclined intrusive sheets and dykes in the Cuillins  
512 volcano, Isle of Skye. In: Pritchard, H.M., Alabaster, T., Harris, N.B., Neary, C.R., (eds),  
513 *Magmatic Processes and Plate Tectonics*, Geological Society, London, *Special Publications*  
514 76, 489-497.
- 515 Walker, R., Healy, D., Kawanzaruwa, T., Wright, K., England, R., McCaffrey, K., Bubeck,  
516 A., Stephens, T., Farrell, N., Blenkinsop, T., 2017. Igneous sills as a record of horizontal

- 517 shortening: The San Rafael subvolcanic field, Utah. Geological Society of America Bulletin  
518 129, 1052-1070.
- 519 Walker, R.J., 2016. Controls on transgressive sill growth. *Geology* 44, 99-102.
- 520 Walsh, J., Bailey, W., Childs, C., Nicol, A., Bonson, C., 2003. Formation of segmented  
521 normal faults: a 3-D perspective. *Journal of Structural Geology* 25, 1251-1262.
- 522 Wilson, P.I., McCaffrey, K.J., Wilson, R.W., Jarvis, I., Holdsworth, R.E., 2016. Deformation  
523 structures associated with the Trachyte Mesa intrusion, Henry Mountains, Utah: Implications  
524 for sill and laccolith emplacement mechanisms. *Journal of Structural Geology* 87, 30-46.
- 525

Figure 1

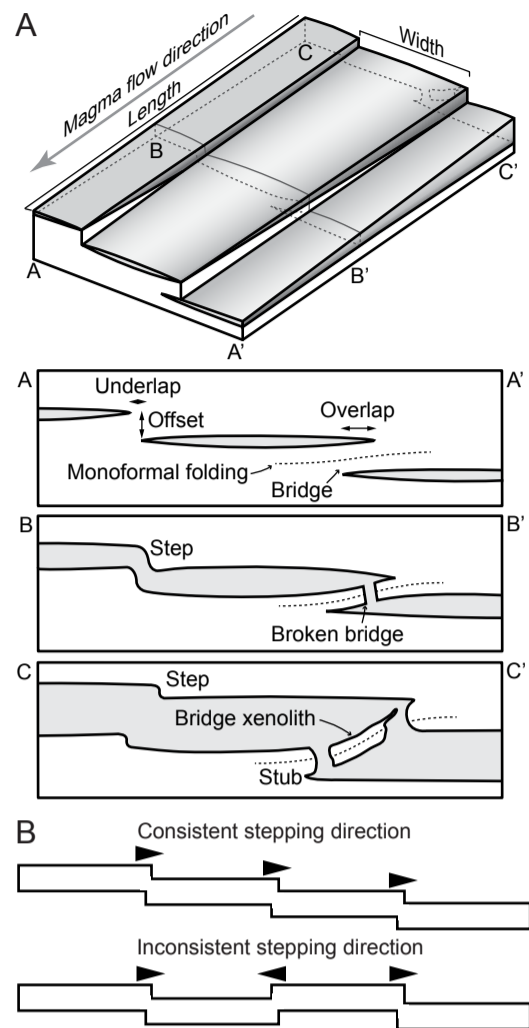


Figure 1: (A) Schematic diagram documenting the description and development of segments connected by steps and bridge structures (redrawn from Magee et al., 2016). (B) Schematic diagram defining consistent and inconsistent stepping directions.



Figure 2

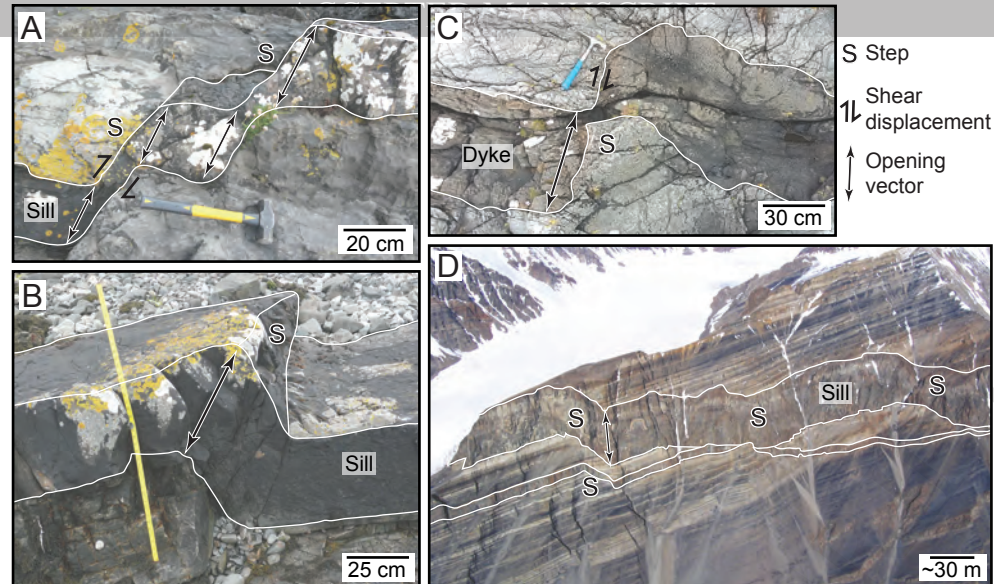


Figure 2: Steps developed in mafic sheets intruding: (A and B) Mesozoic limestone and shale metasedimentary rocks on Ardnamurchan, NW Scotland; (C) Neoproterozoic schists at Mallaig, NW Scotland; and (D) a sedimentary succession on Axel Heiburg island, Canada (photo courtesy of Martin Jackson).

Figure 3

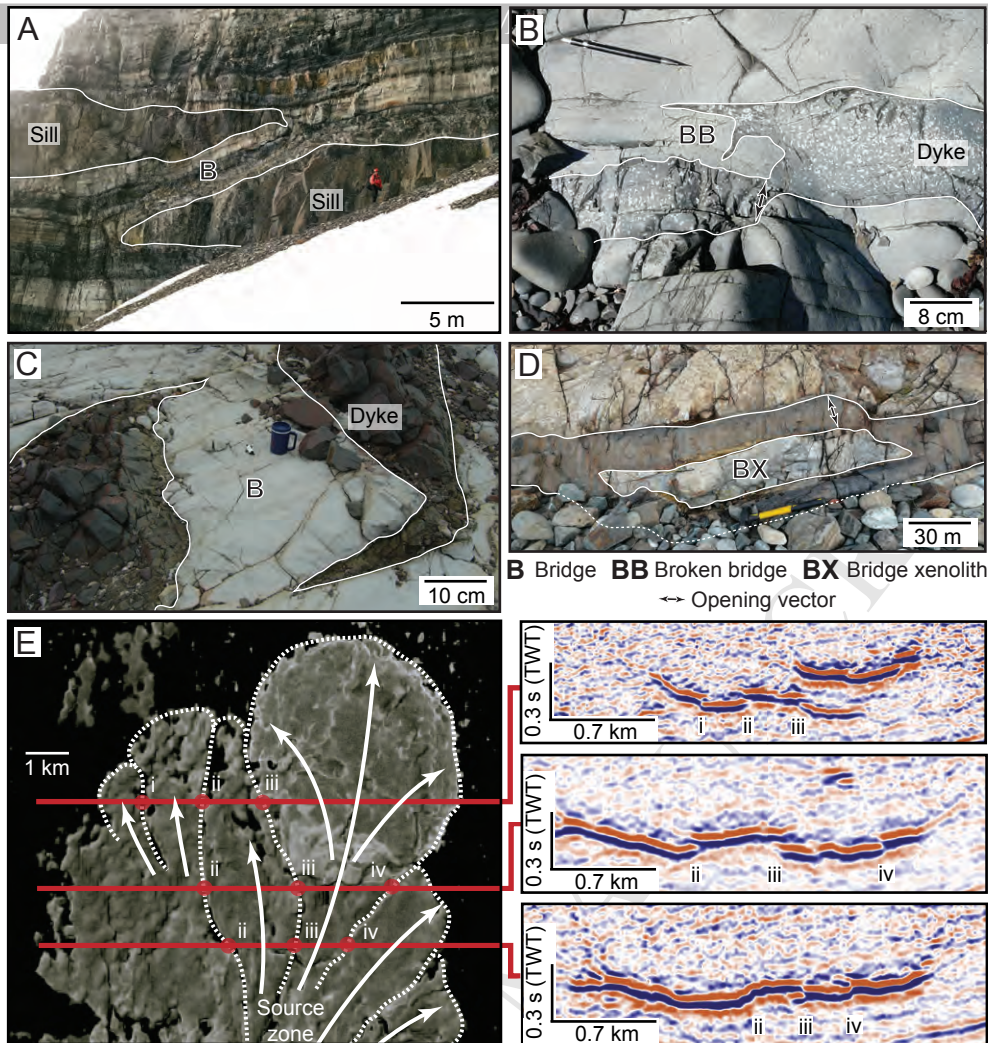


Figure 3: Different bridge structures recorded in mafic intrusions into: (A) Beacon Supergroup sedimentary strata along the Theron Mountains, Antarctica (modified from Hutton, 2009); (B) Beacon Supergroup sedimentary strata along the Allan Hills, Antarctica; (C) a massive dolerite intrusion on Ardnamurchan, NW Scotland; and (D) Mesozoic limestone and shale metasedimentary rocks on Ardnamurchan, NW Scotland. (E) Opacity render of a sill in the Flett Basin, NE Atlantic and corresponding seismic sections detailing intrusive step and bridge growth along i-iv segment boundaries (modified from Schofield et al., 2012b); note that it can be difficult to determine where segments are bounded by steps or bridge structures in seismic reflection data.

Figure 4

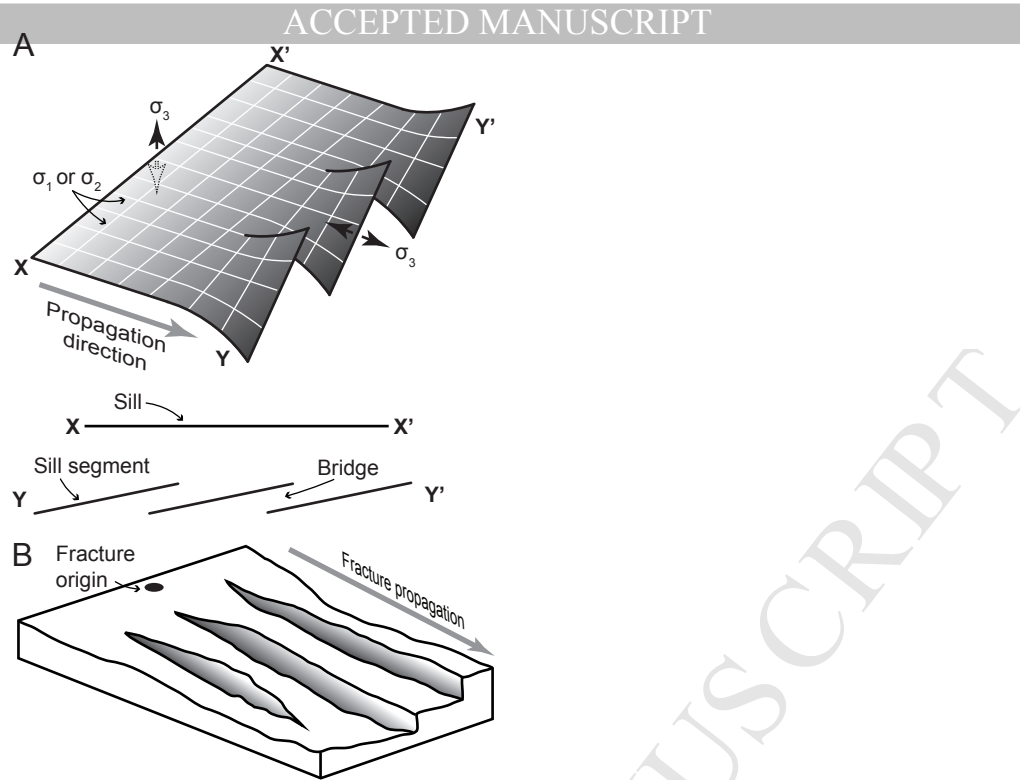


Figure 4: (A) Schematic showing how a change in the principal stress axes can segment a propagating sheet (after Hutton, 2009). (B) Hackle marks developed on a joint plane (redrawn from Kulander et al., 1979).

Figure 5

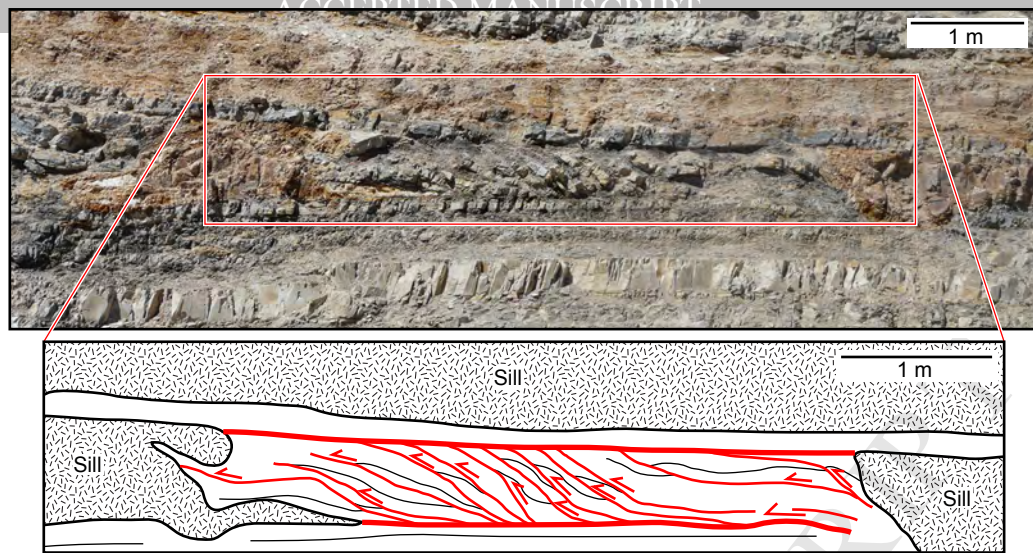


Figure 5: Small-scale imbricate fold and thrust duplex developed due to viscous indentation of finger-like sill intrusions in the Neuquén Basin, Argentina (modified from Spacapan et al., 2017).



Figure 6

ACCEPTED MANUSCRIPT

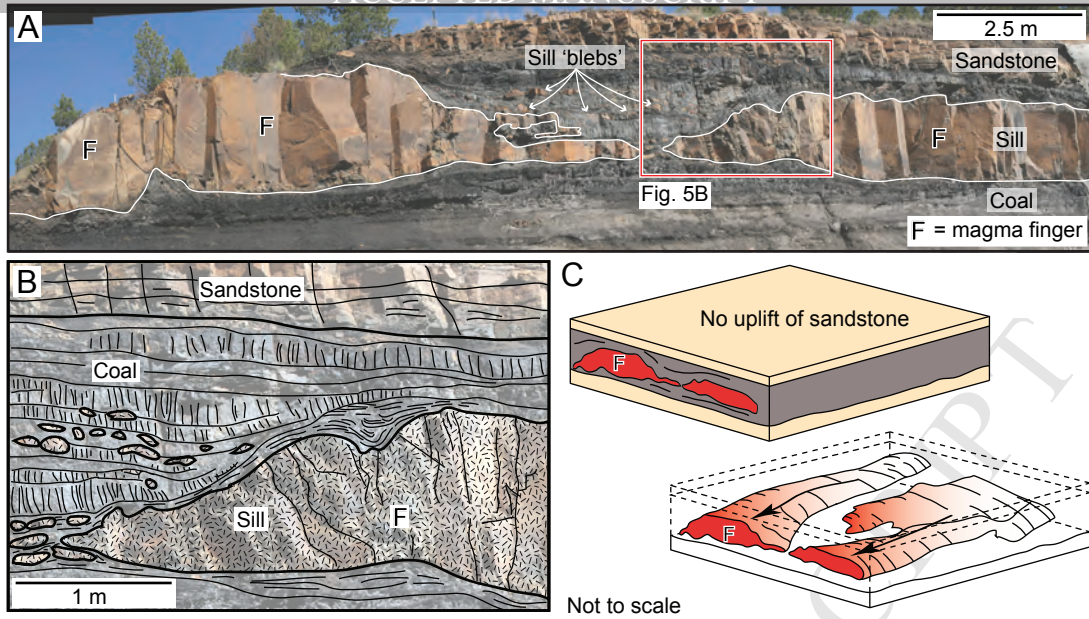


Figure 6: (A and B) Magma fingers developed in response to intrusion-induced heating and plastic deformation of the host rock coals in the Raton Basin, Colorado (modified from Schofield et al., 2012a). (C) Schematic diagrams showing the simplified 3D morphology of the magma fingers in (A and B) (Schofield, 2009).

## Structural signatures of igneous sheet intrusion propagation

Craig Magee<sup>a\*</sup>, James Muirhead<sup>b</sup>, Nick Schofield<sup>c</sup>, Richard Walker<sup>d</sup>, Olivier Galland<sup>e</sup>, Simon Holford<sup>f</sup>, Juan Spacapan<sup>g</sup>, Christopher A-L Jackson<sup>a</sup>, William McCarthy<sup>h</sup>

### Highlights

- 1) Igneous sheet intrusions commonly comprise magma segments (e.g., magma fingers).
- 2) Segments connect via step and bridge structures, formed by brittle fracturing.
- 3) Brittle shear and flow, as well as viscous deformation, can accommodate intrusion.
- 4) Segment long axes form parallel to sheet propagation direction.
- 5) Identifying segments allows magma flow and host rock behaviour to be determined.